Unraveling VPS13A pathways: from Drosophila to human

Pinto, Francesco

CHAPTER 3

Mass spectrometry identified Galectin as a Vps13 interacting protein in *Drosophila*

Francesco Pinto, Liza L. Lahaye, Hjalmar Permentier[1], Marianne van der Zwaag, Sven C. van Ijzendoorn, Ody C.M. Sibon

Manuscript in preparation

Department of Cell Biology, University Medical Center Groningen, University of Groningen, Groningen, the Netherlands.

1. Interfaculty Mass Spectrometry Center (IMSC), University Medical Center Groningen, University of Groningen, Groningen, the Netherlands.

ABSTRACT

ChAc is an autosomal recessive neurodegenerative disorder characterized by neurological features and abnormal red blood cells. The disease is caused by homozygous mutations that occur in the *VPS13A* (Vacuolar protein sorting 13A) gene, which in most cases lead to lower levels or absence of the VPS13A protein in ChAc patients. The cellular function and dynamics of the VPS13A protein are unknown. Determining the protein binding partners and normal functions of VPS13A is necessary to understand molecular mechanisms of ChAc disease. Here, we performed immunoprecipitation coupled to mass spectrometry (IP-MS) in *Drosophila melanogaster* fly heads using control and *Vps13* mutant flies and we identified 53 proteins that potentially interact with the C-terminal region of Vps13. Interaction with Galectin was validated via immunoprecipitation in S2 cells.

INTRODUCTION

Chorea Acanthocytosis (ChAc) is a hereditary neurodegenerative disease caused by the impairment of the VPS13A protein[1]. Chac patients show atrophy of human basal ganglia (especially the head of the caudate, which is a structure of the basal ganglia)[1] and also acanthocytes, star-shaped red blood cells[2]. Characteristic symptoms are abnormal movements including dystonia with tongue protrusion, orofacial dyskinesias, limb dystonia, involuntary vocalizations, dysarthria and involuntary tongue- and lip-biting, cognitive and behaviour changes[3,4]. The disease is incurable and inevitably leads to premature death. The human genome contains four *VPS13* genes, encoding four distinct proteins: VPS13A, VPS13B, VPS13C and VPS13D[5]. Mutations in three of these genes, *VPS13A*, *VPS13B* and *VPS13C* are responsible for the onset of human neurodegenerative diseases, Chorea-Acanthocytosis (ChAc), Cohen syndrome (CS)[6] and Young-onset Parkinson disease (YOPD)[7] respectively.

VPS13A is a conserved protein ranging from yeast to human. In various model organisms, possible functions of VPS13A were identified and a plethora of mutant symptoms were described. In *S. Cerevisiae* the single Vps13 protein is required for proper sporulation and it is involved in trans-Golgi network (TGN) - pre-vacuolar compartment (PVC) trafficking. Furthermore, dominant Vps13 mutations are able to rescue endoplasmatic reticulum-mitochondrial encounter structure (ERMES) mutants, supposing Vps13 can compensate in some way the loss of ERMES[8–10]. In *Tetrahymena termophila,* the Vps13 orthologue is associated with phagosomes and it is involved in phagosomal digestion and formation[11]. *Dictyostelium discoideum* cells lacking Vps13, exhibit a decreased number of autophagosomes and an impaired autophagic degradation[12]. A *VPS13A* knock out model was created in mice and this ChAc mouse model shows increased expression of GABAA1 receptor γ2-subunit and Gephyrin in the striatum and hippocampus[13]. *Drosophila Melanogaster Vps13* mutants show a decreased life span, impaired climbing ability and age-associated neurodegeneration[14]. In addition, *Vps13* mutant flies accumulate ubiquitylated proteins and exhibit increased level of Ref(2)P, the *Drosophila* orthologue of p62, in the central nervous system[14]. ChAc patient's

erythrocytes show impaired autophagy[15] and compromised cytoskeletal architecture[16,17]. In addition, Chorein silenced K562 and rhabdomyosarcoma cells show increased activation of apoptosis[18,19].

Based on the broad phenotypic symptoms listed above, VPS13A may have several independent functions in a specific cell or organism and it may also have redundant roles in different cells and organisms. Despite the fact that VPS13A was identified as the causative gene for ChAc in 2001 and multiple phenotypes have been reported associated with impaired function of VPS13A, little information is available about the cellular processes and pathways in which VPS13A proteins play a role. The identification of proteins that bind or form a complex with VPS13A will help to reveal the cellular function of this protein. To this aim, a high-throughput approach, was applied and immunoprecipitation in combination with mass spectrometry (IP-MS) was used to characterize Vps13 binding partners in head lysates of *Drosophila melanogaster*. IP-MS is a powerful technique that allows to identify potential interactors of a given target and correlated pathways. Fly heads were chosen because in this body part Vps13 was found to be enriched[14].

RESULTS

Identification of Vps13 interactors in fly heads

The *Drosophila melanogaster* genome encodes for three Vps13 proteins, orthologues to Human VPS13A, B and D. In this manuscript we focused on the orthologue of Human VPS13A, further referred to as Vps13. *Drosophila* Vps13 is a peripheral membrane protein containing 3321 amino acids, associated with fractions enriched in endosomal membranes[14]. To perform IP-MS, two fly lines were used: the Bloomington *Drosophila* w^{1118} line and homozygous *Drosophila* $Vps13^{c03628}$ mutants, carrying a PiggyBac transposable element in an intronic region of the *Vps13* gene, as a negative control[20]. Endogenous Vps13 was immunoprecipitated from head lysates of w^{1118} flies, using an antibody (here referred to as NT) binding to the N-terminal region (576-976 aa) of the protein. Lysates of homozygous *Vps13* mutants were used as a negative control.

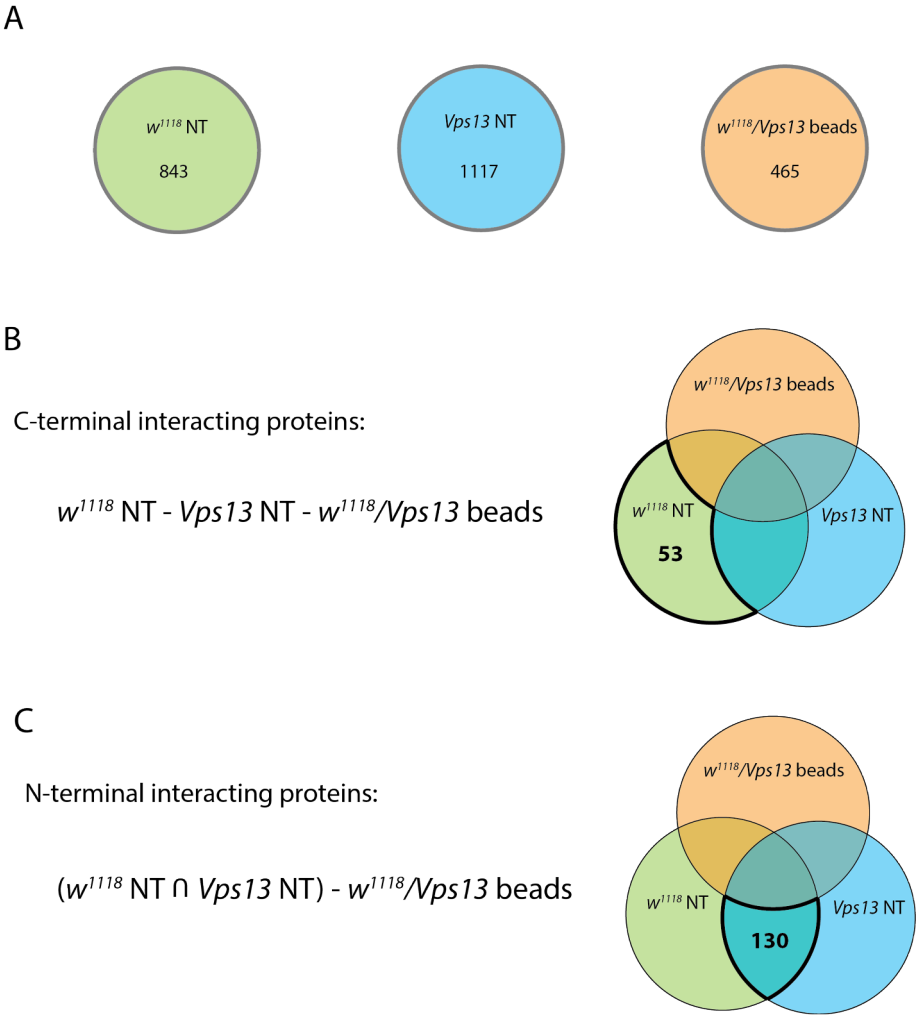

Figure 1. (**A**) Protein hits present in w^{1118} fly heads incubated with the NT ab (w^{1118} NT), *Vps13* mutant fly heads incubated with the NT ab (*Vps13* mutant NT), both w^{1118} and *Vps13* mutant fly heads treated with beads only (w^{1118}/*Vps13* mutant beads). (**B**) and (**C**) A schematic representation of the three sets and their intersection. Proteins exclusively present in "w^{1118} NT" are potential candidates specifically binding to the C-terminal domain (1457-3321 aa) of Vps13. Protein hits present in "w^{1118} NT" and *Vps13* mutant NT" but not in the "w^{1118}/*Vps13* mutant beads" are potential candidates binding to the N terminal part (1-1456 aa) of Vps13. The thick lines indicate the region of the sets containing the proteins binding to the C-terminal and N-terminal part of Vps13.

As additional controls, lysates of heads of *Vps13* mutants and w^{1118} flies incubated with agarose beads without the antibody were used. Immunoblot analysis of the immunoprecipitated fractions showed that Vps13 is enriched in the w^{1118} flies pulldown (Fig. S1). In contrast, and as expected, no full length Vps13 is detected in the pulldown fraction of the *Vps13* mutants nor in the w^{1118} and *Vps13* mutants lysates incubated with the beads without the antibody (Fig. S1). These data demonstrated that endogenous Vps13 can be efficiently immunoprecipitated from fly heads with the used antibody. Immunoprecipitated proteins were in-gel digested, and analzyed and identified by liquid chromatography-tandem mass spectrometry (LC-MS/MS). Surprisingly, we discovered a small amount of truncated Vps13 protein in lysates of *Vps13* mutant flies. This truncated Vps13 protein, lacking the C-terminal half, is consistent with the position of the PiggyBac insertion (after 1456 aa) (Fig. S2B) and indicates that homozygous *Vps13* mutants express low levels of a truncated protein. Therefore, it is possible that in the immunoprecipitated fraction of the negative control (heads of *Vps13* mutants), which contains the truncated protein, Vps13 N-terminal binding partners are present. The proteins are grouped in three sets (Fig. 1): w^{1118} fly heads incubated with the NT ab (w^{1118} NT), *Vps13* mutant fly heads incubated with the NT ab (*Vps13* mutant NT), w^{1118} and *Vps13* mutant fly heads treated with beads only (w^{1118}/*Vps13* mutant beads). Thus, two lists of potential Vps13 interactors are created; the first, which is referred as C-terminal (1457-3321 aa) binding list, contains the proteins present in w^{1118} NT, absent in *Vps13* mutant NT and absent in w^{1118}/*Vps13* mutant beads. This list includes 53 proteins and is the most selective and reliable group as it excludes proteins that bind to the NT antibody in a non-specific manner. Importantly, potential N-terminal (1-1456 aa) binding proteins present in *Vps13* mutant NT set are excluded from this list, therefore proteins present in this list are likely interactors of the C-terminal of Vps13 (Table 1). The second list, referred as N-terminal binding, includes proteins shared between w^{1118} NT and *Vps13* mutant NT sets and absent in w^{1118}/*Vps13* mutant beads. The N-terminal binding list contains 130 proteins and this list is less accurate, because non-specific proteins recognized by the NT ab may be present in this group (Table S3). In this study we focus mainly on the C-terminal list.

N	Annotation symbol	Symbol	Name	-10lgP	Cov. %	Pep
1	CG9244	Acon	Aconitase	382.92	42	22
2	CG6186	Tsf1	Transferrin1	380.54	40	22
3	CG11372	Galectin	Galectin	363.16	48	20
4	CG6058	Ald	Aldolase	344.87	49	18
5	CG3731	UQCR-C1	Ubiquinol-cytochrome c reductase core protein 1	242.57	26	6
6	CG34417	CG34417	no name	239.61	10	5
7	CG7998	Mdh2	Malate dehydrogenase 2	237.72	35	6
8	CG6647	Porin	Porin	236.50	34	7
9	CG5320	Gdh	Glutamate dehydrogenase	234.91	21	9
10	CG17654	Eno	Enolase	230.17	16	3
11	CG9261	nrv2	nervana 2	225.39	28	5
12	CG7399	Hn	Henna	210.77	15	5
13	CG2184	Mlc2	Myosin light chain 2	204.90	25	3
14	CG3011	Shmt	Serine hydroxymethyl transferase	198.29	14	4
15	CG2286	ND75	NADH dehydrogenase (ubiquinone) 75 kDa subunit	192.97	8	4
16	CG15848	Scp1	Sarcoplasmic calcium-binding protein 1	191.86	26	4
17	CG1970	ND-49	NADH dehydrogenase (ubiquinone) 49 kDa subunit	189.91	14	4
18	CG6988	Pdi	Protein disulfide isomerase	187.64	15	6
19	CG8256	Gpo-1	Glycerophosphate oxidase-1	184.45	11	4
20	CG5594	kcc	kazachoc	180.44	4	4
21	CG4600	yip2	yippee interacting protein 2	180.09	22	5
22	CG5177	CG5177	no name	176.83	20	3

23	CG1469	Fer2LCH	Ferritin 2 light chain homologue	171.76	26	3
24	CG15811	Rop	Ras opposite	171.36	7	3
25	CG9042	Gpdh	Glycerol 3 phosphate dehydrogenase	166.41	19	5
26	CG2204	Gαo	G protein α o subunit	161.39	15	4
27	CG31196	14-3-3epsilon	14-3-3ε	159.87	23	3
28	CG8996	wal	walrus	155.73	11	2
29	CG1417	SlgA	sluggish A	155.11	8	3
30	CG12101	Hsp60	Heat shock protein 60A	154.25	8	3
31	CG6783	fabp	fatty acid binding protein	149.13	38	3
32	CG7433	Gabat	γ-aminobutyric acid transaminase	141.47	7	3
33	CG7361	RFeSP	Rieske iron-sulfur protein	139.57	22	4
34	CG1065	Scsα	Succinyl coenzyme A synthetase α subunit	137.63	13	3
35	CG7176	Idh	Isocitrate dehydrogenase	132.99	10	4
36	CG13279	cyt-B5-r	Cytochrome b5-related	129.95	7	2
37	CG1618	comt	comatose	127.53	6	3
38	CG1732	Gat	GABA transporter	123.44	7	3
39	CG11739	Sfxn1-3	Sideroflexin 1/3	122.43	9	2
40	CG14994	Gad1	Glutamic acid decarboxylase 1	122.41	7	2
41	CG15825	fon	fondue	121.46	7	2
42	CG5889	Men-b	Malic enzyme b	118.20	4	2
43	CG7430	CG7430	no name	115.59	5	2
44	CG7834	CG7834	no name	113.41	11	2
45	CG6518	inaC	inactivation no afterpotential C	112.06	3	2
46	CG16884	CG16884	no name	102.07	10	2

47	CG6020	ND-39	NADH dehydrogenase (ubiquinone) 39 kDa subunit	99.11	11	2
48	CG6781	se	sepia	98.77	9	2
49	CG3244	Clect27	C-type lectin 27kD	93.85	12	2
50	CG9394	CG9394	no name	83.03	4	2
51	CG7269	Hel25E	Helicase at 25E	82.81	5	2
52	CG1721	Pglym78	Phosphoglyceromutase	78.85	10	2
53	CG46149	Fatp	Fatty acid (long chain) transport protein	58.30	3	2

Table 1. List of proteins binding to the C-terminal part of Vps13. The proteins are listed in order of decreasing PEAKS Protein Score (-10logP). The number of supporting peptides and the percentage of protein coverage are listed.

An enrichment analysis of the Vps13-interacting proteins from Table 1 was applied in the Gene Ontology (GO) domain "Cellular Component". The top five results are shown in Table 2. Interestingly the first two components are lipid particle and mitochondrion; these data are consistent with chapter 4 in which it was demonstrated that human VPS13A is able to bind mitochondria and lipid droplets, however the binding partners were not identified in chapter 4. Further analysis in the Gene Ontology domains "Molecular Function" and "Biological Process" were performed and shown in Table S1 and Table S2.

Vps13 interacts with Galectin

One of the proteins identified with a high score (an indication for a relatively high abundance) in the C-terminal binding list was Galectin. Galectins are a family of proteins able to bind β-galactoside sugars. They are conserved in mammals, fish, birds, insects, fungi and more[22,23]. Until now, 15 galectins were discovered in mammals, encoded by the *LGALS* genes. They are involved in different functions including cell–cell interactions, cell–matrix adhesion, transmembrane signaling, apoptosis and others[23,24]. In humans 10 Galectin proteins are present and they are expressed in a wide range of tissues. Human Vps13C was found to interact with Galectin-12 in adipocytes[25].

#pathway ID	Pathway description	Observed gene count	%	false discovery rate
GO.0005811	lipid particle	17	32,1	9.94e-16
GO.0005739	mitochondrion	22	41,5	5,00E-14
GO.0044444	cytoplasmic part	34	64,2	5,00E-14
GO.0005737	cytoplasm	37	69,8	5.94e-13
GO.0005623	cell	47	88,7	2.9e-11

Table 2. Enriched GO Cellular Component terms. C-terminal interacting proteins were tested for GO Cellular Component using String database version 10.5[21]. Pathways are listed based on the false discovery rate. Observed gene count and percentage of the total are listed.

In *Drosophila* only one Galectin protein is known. The *Drosophila* Galectin is very abundant in embryonic and larval tissue but it is also expressed in visceral musculature, in the central nervous system and hemocytes. Thus, *Drosophila* Galectin may be involved in cell-cell communication, innate immune system and cross-linking of receptors to trigger signal transduction events[26].

Because of the interaction of human VPS13C with Galectin, we investigated further the possible interaction between *Drosophila* Vps13 and Galectin. To validate the interaction between Vps13 and Galectin, a GFP-Galectin fusion protein and GFP as control were overexpressed in *Drosophila* S2 cultured cells; subsequently, a pulldown using GFP-Trap was executed. GFP and GFP-Galectin are efficiently immunoprecipitated in both samples; Vps13 was enriched only in the GFP-Galectin sample but not in the GFP sample, indicating an interaction between Vps13 and Galectin (Fig.2).

DISCUSSION

ChAc is a neurodegenerative disease caused by the loss of function of VPS13A. The mechanisms that lead to the onset of this disorder are still not known. In this study we use *Drosophila melanogaster* as a model and we applied IP–MS in fly heads to identify Vps13 interactors to gain insight into possible pathways in which Vps13 could play a role. Here, we show 2 different lists of potential proteins interacting with the N-terminal (1-1456 aa) or C-terminal (1457-3321 aa) part of Vps13. Human Vps13A is associated with mitochondria and lipid droplets (chapter 4), however proteins necessary to bind these organelles are still unknown.

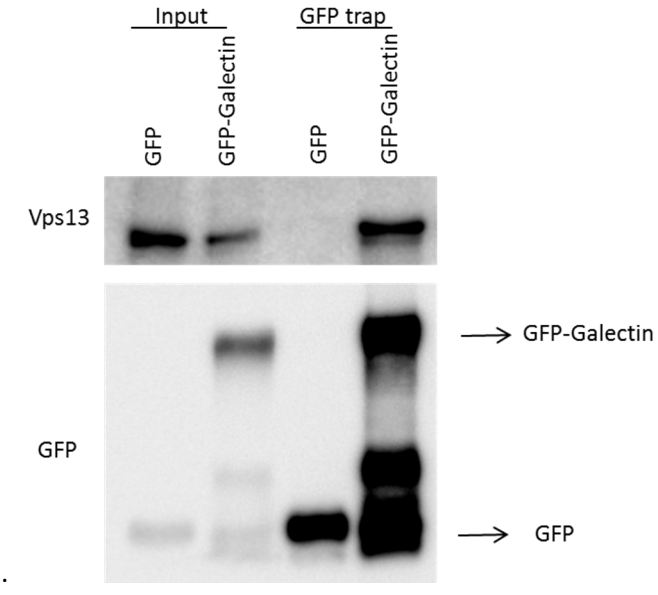

Figure 2. GFP-Galectin and free GFP, overexpressed in S2 cells, are immunoprecipitated using GFP-Trap. The arrows indicated the bands of GFP and GFP-Galectin.

Several mitochondrial and lipid droplet-associated proteins were identified in our IP-MS analysis, and these players can be starting points for further research to understand the possible function of VPS13A at these various organelles. Human Vps13C was found to interact with Galectin-12 in adipocytes, this interaction is stabilizing Galectin-12, preventing lysosomal degradation and Galectin-12 stability is crucial for adipocyte differentiation[25]. In contrast to humans, there is only one Galectin protein in *Drosophila* and it has been reported that it is indeed expressed in fly heads[27]. *Drosophila* Galectin is also present on the surface of muscles and it is necessary for axon guidance and synaptogenesis[28], suggesting a possible role for Galectin in essential functions and processes of the nervous system as well. In addition, some Human Galectin proteins are involved in neurodegeneration controlling microglia-mediated neurotoxicity[29] or promoting neuroprotection decreasing the expression of inflammatory molecules[30]. These results suggest a possible functional role of the interaction of Vps13-Galectin in the onset and development of neurodegeneration in ChAc disease. In conclusion our study shows an interesting selection of possible binding candidates of Vps13, providing valuable information for directions for future research. *Drosophila*

melanogaster can be a suitable model to further investigate the interaction Vps13-Galectin. Additional experiments need to be done to demonstrate a possible involvement of this interaction in the pathophysiology of ChAc.

MATERIAL AND METHODS

Fly stocks

Fly stocks were maintained at 25 °C on standard agar food. The *Vps13*^{c03628} stock was acquired from the Exelixis stock centre[31]. The *Vps13*^{c03628} stock was isogenized to the *w*^{1118} stock. The generation of the isogenic controls was performed as previously described[32]. In short, The isogenic fly lines that serve as a control were generated by backcrossing the *Vps13* mutant line for 6 generations with the control stock (*w*^{1118}). The *w*^{1118} stock was acquired from the Bloomington Stock Centre.

Western blot analysis

Samples were boiled at 99 ^{o}C for 5 minutes, the proteins were resolved with polyacrylamide gel and transferred to PVDF membrane using the Trans-Blot Turbo System (Bio-Rad) or overnight wet transfer. Membranes blocked in 5% fat free milk for 1 hour at room temperature, rinsed in PBS-Tween 20. Incubations with primary antibodies were done overnight at 4 ^{o}C followed by incubations with secondary antibodies for 1 hour at room temperature. The following primary antibodies were used: anti-dVps13NT (1:1000), anti-dVps13(62) (1:1000), anti-GFP (Clontec 1:1000). Membrane was developed using ECL reagent (Thermo Scientific) and signal was imaged using the ChemiDoc imager (Bio-Rad).

Immunoprecipitation

Fly heads were collected and resuspended in 2 µl of lysisbuffer per head (1% NP40, 0,5% DOC, 10% glycerol, 1mM sodium orthovanadate, 5 mM sodium fluoride in PBS supplemented with protease inhibitor cocktail, Roche). The samples were sonicated 3 times per 5 seconds. The samples were centrifuged for 20 min at 4 C at 20000 g and the supernatants were collected and subjected to overnight immunoprecipitation using Vps13 NT antibody. 30 µl of

Protein A/G slurry beads (santacruz) were equilibrated in wash buffer (5 washes) and added to each of the sample at 4 C for 1 hr. The beads were washed 5 times in 500 µl of ice cold lysisbuffer buffer and were eluted in 100 µl of 2x SDS-sample buffer. Equal amounts of volume were processed for Western blot and Mass Spectrometry analysis.

LC MS/MS

Protein samples were reduced with 10 mM DTT at 56 °C for 30 min, and alkylated with 55 mM iodoacetamide at room temperature in the dark for 30 min. Tryptic digestions were performed at 37 °C overnight. LC-MS/MS of the tryptic peptides was performed using an Ultimate 3000 nano-UPLC system (Thermo Fisher Scientific) coupled to a Q Exactive plus mass spectrometer with a NanoFlex source (Thermo Fisher Scientific) equipped with a stainless steel emitter. Samples were loaded onto a 5 mm × 300 µm i.d. Acclaim C18 PepMap 100 5 µm trapping microcolumn (Thermo) in 0.1% FA at a flow rate of 20 µL/min. Trapped peptide were separated on a 25 cm × 75 µm i.d. Acclaim C18 PepMap 100 2 µm column (Thermo). A mobile phase gradient was delivered at the flow rate of 300 nL/min, increasing the acetonitrile concentration from 2% to 40% in water with 0.1% formic acid. MS and MS/MS data were acquired using a data-dependent top-10 method choosing the 10 most abundant precursor ions from the MS survey scans (300–1650 Th) with a dynamic exclusion time of 20 s. Peptide MS/MS spectra were obtained via fragmentation by high energy collisional dissociation (HCD). Survey scans were acquired at a resolution of 70,000 at m/z 200. The resolution for HCD spectra was set to 17,500 at m/z 200 with a maximum ion injection time of 100 ms. The normalized collision energy was set at 27. Precursor ions with single, unassigned, or seven and higher charge states were excluded from fragmentation selection. PEAKS 7 software (Bioinformatics Solutions Inc., Waterloo, Ontario, Canada) was used to search the MS/MS spectra against a *Drosophila melanogaster* protein database (Uniprot reference proteome, 1-2015), allowing for the variable oxidation of Met (+15.99 Da), fixed modification of Cys (+57.02 Da), up to 3 missed cleavages, a parent mass error tolerance of 10 or 15 ppm and a fragment mass error tolerance of 0.02 or 0.04 Da. The false discovery rate was set at 0.1% at the peptide level.

GFP-TRAP assay

For one immunoprecipitation reaction one T75 flask of S2 cells was used. The cells were resuspended in 200 µl of ice cold lysis buffer (10 mM Tris/Cl pH 7.5; 150 mM NaCl; 0.5 mM EDTA; 0,5% NP-40) and placed on ice for 30 min, extensively pipetting every 10 min. Cell lysate was centrifuged at 20000x g for 10 min at 4 °C and the supernatant was added in a new tube which contained 300 µl of dilution/wash buffer (10 mM Tris/Cl pH 7.5; 150 mM NaCl; 0.5 mM EDTA). 25 µl of GFP-TRAP_A beads (chromotek) were equilibrated in wash buffer (5 washes) and added to each of the diluted sample. The mixture was rotated for 1 hour at 4 °C. GFP-TRAP_A beads were washed 5 times in 500 µl of ice cold dilution/wash buffer. The beads were eluted in 100 µl of 2x SDS-sample buffer and equal amounts of volume were processed for Western blot analysis.

REFERENCES

1. Prohaska, R. *et al.* Brain, blood, and iron: Perspectives on the roles of erythrocytes and iron in neurodegeneration. *Neurobiol. Dis.* **46,** 607–624 (2012).

2. Sorrentino, G., De Renzo, A., Miniello, S., Nori, O. & Bonavita, V. Late appearance of acanthocytes during the course of chorea-acanthocytosis. *J. Neurol. Sci.* **163,** 175–8 (1999).

3. Fontenelle, L. F. & Leite, M. A. A. Treatment-resistant self-mutilation, tics, and obsessive-compulsive disorder in neuroacanthocytosis: a mouth guard as a therapeutic approach. *J. Clin. Psychiatry* **69,** 1186–7 (2008).

4. Benninger, F. *et al.* Seizures as presenting and prominent symptom in chorea-acanthocytosis with c.2343del VPS13A gene mutation. *Epilepsia* **57,** 549–556 (2016).

5. Velayos-Baeza, A., Vettori, A., Copley, R. R., Dobson-Stone, C. & Monaco, A. P. Analysis of the human VPS13 gene family. *Genomics* **84,** 536–549 (2004).

6. Seifert, W. *et al.* Cohen syndrome-associated protein, COH1, is a novel, giant Golgi matrix protein required for Golgi integrity. *J. Biol. Chem.* **286,** 37665–75 (2011).

7. Lesage, S. *et al.* Loss of VPS13C Function in Autosomal-Recessive Parkinsonism Causes Mitochondrial Dysfunction and Increases PINK1/Parkin-Dependent Mitophagy. *Am. J. Hum. Genet.* **98,** 500–513 (2016).

8. Park, J.-S. *et al.* Yeast Vps13 promotes mitochondrial function and is localized at membrane contact sites. *Mol. Biol. Cell* **27,** 2435–2449 (2016).

9. Lang, A. B., John Peter, A. T., Walter, P. & Kornmann, B. ER-mitochondrial junctions can be bypassed by dominant mutations in the endosomal protein Vps13. *J. Cell Biol.* **210,** 883–90 (2015).

10. John Peter, A. T. *et al.* Vps13-Mcp1 interact at vacuole–mitochondria interfaces and bypass ER–mitochondria contact sites. *J. Cell Biol.* **216,** 3219–3229 (2017).

11. Samaranayake, H. S., Cowan, A. E. & Klobutcher, L. A. Vacuolar protein sorting protein 13A, TtVPS13A, localizes to the Tetrahymena thermophila phagosome membrane and is required for efficient phagocytosis. *Eukaryot. Cell* **10,** 1207–1218 (2011).

12. Muñoz-Braceras, S., Calvo, R. & Escalante, R. TipC and the chorea-acanthocytosis protein VPS13A regulate autophagy in Dictyostelium and human HeLa cells. *Autophagy* **11,** 918–927 (2015).

13. Kurano, Y. *et al.* Chorein deficiency leads to upregulation of gephyrin and GABA(A) receptor. *Biochem. Biophys. Res. Commun.* **351,** 438–442 (2006).

14. Vonk, J. J. *et al.* Drosophila Vps13 is required for protein homeostasis in the brain. *PLoS One* **12,** 1–21 (2017).

15. Lupo, F. *et al.* A new molecular link between defective autophagy and erythroid abnormalities in chorea-acanthocytosis. *Blood* **128,** 2976–2987 (2016).

16. Honisch, S. *et al.* Chorein Sensitive Arrangement of Cytoskeletal Architecture. *Cell. Physiol. Biochem.* **37,** 399–408 (2015).

17. De Franceschi, L. *et al.* Erythrocyte membrane changes of chorea-acanthocytosis are the result of altered Lyn kinase activity. *Blood* **118,** 5652–63 (2011).

18. Föller, M. *et al.* Chorein-sensitive polymerization of cortical actin and suicidal cell death in chorea-acanthocytosis. *FASEB J.* **26,** 1526–1534 (2012).

19. Honisch, S. *et al.* Chorein addiction in VPS13A overexpressing rhabdomyosarcoma cells. *Oncotarget* **6,** 10309–10319 (2015).

20. Vonk, J. J. *et al.* Drosophila Vps13 Is Required for Protein Homeostasis in the Brain. 1–21 (2017). doi:10.1371/journal.pone.0170106

21. Szklarczyk, D. *et al.* STRING v10: protein–protein interaction networks, integrated over the tree of life. *Nucleic Acids Res.* **43,** (2015).

22. Cooper, D. N. W. & Barondes, S. H. God must love galectins; he made so many of them. *Glycobiology* **9,** 979–84 (1999).

23. Cummings, R. D. & Liu, F.-T. *Galectins*. *Essentials of Glycobiology* (Cold Spring Harbor Laboratory Press, 2009).

24. Barondes, S. H., Cooper, D. N., Gitt, M. A. & Leffler, H. Galectins. Structure and function of a large family of animal lectins. *J. Biol. Chem.* **269,** 20807–10 (1994).

25. Yang, R.-Y. *et al.* Identification of VPS13C as a Galectin-12-Binding Protein That Regulates Galectin-12 Protein Stability and Adipogenesis. *PLoS One* **11,** e0153534 (2016).

26. Pace, K. E. *et al.* Characterization of a Novel Drosophila melanogaster Galectin. *J. Biol. Chem.* **277,** 13091–13098 (2002).

27. Aradska, J. *et al.* Gel-free mass spectrometry analysis of Drosophila melanogaster heads. *Proteomics* **15,** 3356–3360 (2015).

28. Kurusu, M. *et al.* A Screen of Cell-Surface Molecules Identifies Leucine-Rich Repeat Proteins as Key Mediators of Synaptic Target Selection. *Neuron* **59,** 972–985 (2008).

29. Starossom, S. C. *et al.* Galectin-1 Deactivates Classically Activated Microglia and Protects from Inflammation-Induced Neurodegeneration. *Immunity* **37,** 249–263 (2012).

30. Yip, P. K. *et al.* Galectin-3 released in response to traumatic brain injury acts as an alarmin orchestrating brain immune response and promoting neurodegeneration. *Sci. Rep.* **7,** 41689 (2017).

31. Thibault, S. T. *et al.* A complementary transposon tool kit for Drosophila melanogaster using P and piggyBac. *Nat. Genet.* **36,** 283–287 (2004).

32. Burnett, C. *et al.* Absence of effects of Sir2 overexpression on lifespan in C. elegans and Drosophila. *Nature* **477,** 482–485 (2011).

SUPPLEMENTARY FIGURES

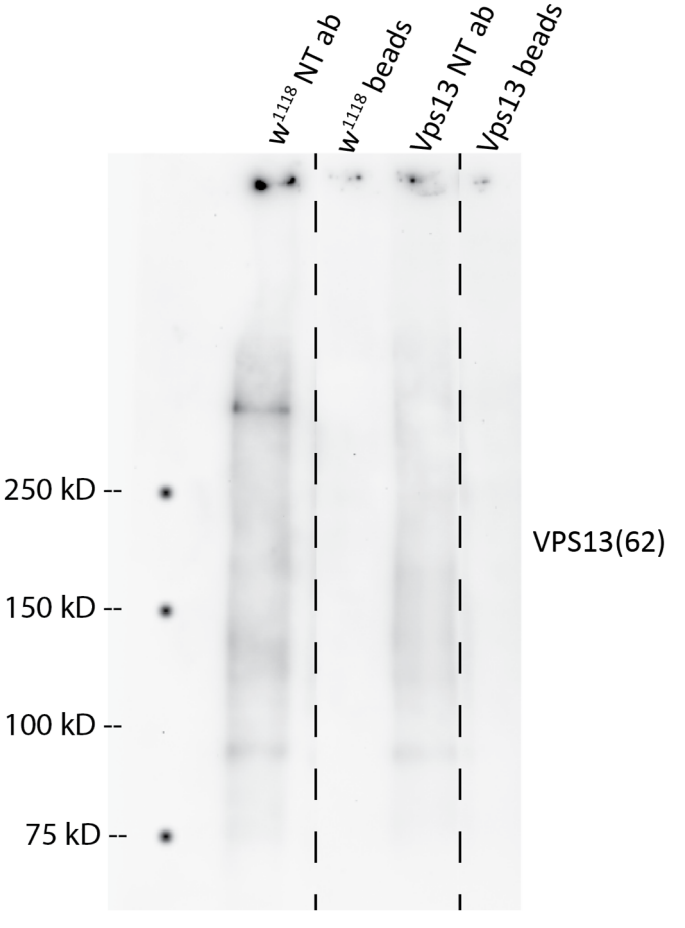

Figure S1. Western blot of the four samples used for the IP-MS. Vps13 band is visible only in w^{1118} NT ab. For the detection Vps13(62) ab, binding a C-terminal epitope of the protein, was used.

A

B

Figure S2. Coverage of Vps13 protein in w^{1118} NT (**A**) and *Vps13* mutant NT (B). The underlined sequences indicate the tryptic peptides detected by LC-MS/MS, with a significant identifcation score. Amino acids with modifications are highlighted: red spots represent oxidized methionine, yellow spots represent carbamidomethylated cysteine. *Vps13* mutant flies (**B**) show supporting peptides only in the N-terminal region preceding the PiggyBac insertion.

#pathway ID	pathway description	observed gene count	%	false discovery rate
GO.0048037	cofactor binding	12	22,6	4.55e-09
GO.0016491	oxidoreductase activity	15	28,3	9.82e-07
GO.0003824	catalytic activity	32	60,4	1.26e-05
GO.0050662	coenzyme binding	8	15,1	1.62e-05
GO.0005488	binding	33	62,3	8.34e-05

Table S1. Enriched GO Molecular Function terms. C-terminal interacting proteins were tested for GO Molecular Function using String database version 10.5[21]. Pathways are listed based on the false discovery rate. Observed gene count and percentage of the total are also showed.

#pathway ID	pathway description	observed gene count	%	false discovery rate
GO.0006091	generation of precursor metabolites and energy	16	30,2	2.04e-15
GO.0044281	small molecule metabolic process	22	41,5	1.03e-12
GO.0045333	cellular respiration	12	22,6	3.24e-11
GO.0055114	oxidation-reduction process	16	30,2	1.01e-08
GO.0009117	nucleotide metabolic process	12	22,6	3.51e-08

Table S2. Enriched GO Biological Process terms. C-terminal interacting proteins were tested for GO Biological Process using String database version 10.5[21]. Pathways are listed based on the false discovery rate. Observed gene count and percentage of the total are also showed.

N	Annotation symbol	Symbol	Name	-10lgP	Cov %	Pep
1	CG2918	CG2918	no name	478.95	40	28
2	CG3523	FAS	Fatty acid synthase 1	454.14	26	40
3	CG8092	Row	relative of woc	421.47	29	27
4	CG5965	Woc	without children	393.76	17	22
5	CG9373	Rump	rumpelstiltskin	385.08	32	20
6	CG1744	Chp	chaoptin	362.96	20	18
7	CG32498	Dnc	dunce	352.89	18	14
8	CG3481	Adh	Alcohol dehydrogenase	344.28	59	11
9	CG1242	Hsp83	Heat shock protein 83	342.88	29	15
10	CG18102	Shi	shibire	320.30	22	13
11	CG7470	CG7470	no name	303.91	24	13
12	CG7254	GlyP	Glycogen phosphorylase	303.67	21	13
13	CG3861	kdn	knockdown	301.96	31	11
14	CG1873	Ef1alpha100E	eukaryotic translation elongation factor 1 alpha 2	297.71	40	17
15	CG2238	EF2	eukaryotic translation elongation factor 2	291.68	20	12
16	CG42310	Prom	prominin	291.43	12	12
17	CG10844	Rya-r44F	Ryanodine receptor	286.50	4	16
18	CG30084	Zasp52	Z band alternatively spliced PDZ-motif protein 52	286.36	9	12
19	CG4863	Rpl3	Ribosomal protein L3	284.82	36	14
20	CG12403	Vha68-1	Vacuolar H+ ATPase 68kD subunit 1	274.34	25	9
21	CG17369	Vha55	Vacuolar H+-ATPase 55kD subunit	269.16	25	8

22	CG4260	AP-2alpha	Adaptor Protein complex 2, α subunit	257.74	10	7
23	CG2331	TER94	TER94	254.36	19	8
24	CG7070	Pyk	Pyruvate kinase	254.29	21	8
25	CG9441	Pu	Punch	252.62	36	11
26	CG4994	Mpcp	Mitochondrial phosphate carrier protein 2	247.71	31	11
27	CG6871	Cat	Catalase	241.16	22	6
28	CG34417	CG34417	no name	239.61	2	5
29	CG5962	Arr2	Arrestin 2	235.65	30	8
30	CG11963	skap	skpA associated protein	235.03	21	5
31	CG7610	ATPsyn-gamma	ATP synthase, γ subunit	231.67	23	6
32	CG7490	RpLP0	Ribosomal protein LP0	231.58	28	6
33	CG5119	pAbp	poly(A) binding protein	228.86	14	7
34	CG42492	CG42492	no name	226.67	9	4
35	CG8251	Pgi	Phosphoglucose isomerase	226.67	13	6
36	CG5920	RpS2	Ribosomal protein S2	225.23	35	7
37	CG42540	CG42540	no name	222.51	19	5
38	CG6143	Pep	Protein on ecdysone puffs	221.88	14	7
39	CG4464	RpS19a	Ribosomal protein S19a	220.12	46	6
40	CG1475	RpL13A	Ribosomal protein L13A	219.89	41	10
41	CG3762	Vha68-2	Vacuolar H+ ATPase 68 kDa subunit 2	218.22	16	6
42	CG3203	RpL17	Ribosomal protein L17	217.87	26	5
43	CG10305	RpS26	Ribosomal protein S26	216.87	32	4
44	CG7977	RpL23a	Ribosomal protein L23A	216.61	27	7

45	CG17870	14-3-3zeta	14-3-3ζ	216.04	19	4
46	CG8322	ATPCL	ATP citrate lyase	214.77	8	5
47	CG12262	CG12262	no name	214.74	19	6
48	CG6439	Idh	Isocitrate dehydrogenase 3b	213.94	21	6
49	CG17838	Syp	Syncrip	213.72	23	9
50	CG17489	RpL5	Ribosomal protein L5	213.70	31	8
51	CG10119	LamC	Lamin C	211.26	15	6
52	CG4897	RpL7	Ribosomal protein L7	210.05	27	7
53	CG5390	CG5390	no name	202.33	10	4
54	CG6782	sea	scheggia	199.59	23	7
55	CG8201	par-1	par-1	198.95	9	6
56	CG1263	RpL8	Ribosomal protein L8	198.48	24	4
57	CG6203	Fmr1	Fmr1	192.33	9	4
58	CG6815	bor	belphegor	191.50	10	5
59	CG6510	RpL18a	Ribosomal protein L18A	188.15	42	6
60	CG42309	Mlp60A	Muscle LIM protein at 60A	187.92	61	4
61	CG2145	CG2145	no name	186.58	10	4
62	CG3299	Vinc	Vinculin	186.53	8	6
63	CG12775	RpL21	Ribosomal protein L21	184.78	37	4
64	CG42734	Ank2	Ankyrin 2	182.91	4	8
65	CG4001	Pfk	Phosphofructokinase	182.82	8	4
66	CG34387	futsch	futsch	182.20	1	5
67	CG9297	CG9297	no name	182.20	5	5
68	CG6416	Zasp66	Z band alternatively spliced PDZ-motif protein 66	180.16	17	5

69	CG8663	nrv3	nervana 3	179.65	13	4
70	CG12749	Hrb87F	Heterogeneous nuclear ribonucleoprotein at 87F	179.53	14	4
71	CG9674	CG9674	no name	177.79	4	5
72	CG1316	CG1316	no name	177.08	11	4
73	CG6141	RpL9	Ribosomal protein L9	177.02	25	4
74	CG11876	CG11876	no name	176.19	10	3
75	CG9432	l(2)01289	lethal (2) 01289	174.10	4	4
76	CG4581	Thiolase	Thiolase	173.20	12	4
77	CG15693	RpS20	Ribosomal protein S20	172.29	36	4
78	CG1021	Dmtn	Dementin	171.05	14	5
79	CG5014	Vap-33A	VAMP-associated protein 33kDa	170.30	23	3
80	CG12532	AP-1-2beta	Adaptor Protein complex 1/2, β subunit	164.72	5	4
81	CG5028	CG5028	no name	161.23	13	4
82	CG3989	ade5	ade5	159.22	11	4
83	CG8189	ATPsyn-b	ATP synthase, subunit B	151.45	11	2
84	CG1106	Gel	Gelsolin	151.06	5	4
85	CG34069	COX2	mitochondrial Cytochrome c oxidase subunit II	150.16	16	2
86	CG7057	AP-2mu	Adaptor Protein complex 2, μ subunit	149.51	6	3
87	CG13057	retinin	retinin	145.19	24	3
88	CG2033	RpS15Aa	Ribosomal protein S15Aa	144.58	27	3
89	CG17759	Gαq	G protein α q subunit	144.08	11	3
90	CG7010	l(1)G0334	lethal (1) G0334	143.01	11	2
91	CG30122	CG30122	no name	142.10	4	2

92	CG10664	COX4	Cytochrome c oxidase subunit 4	140.83	32	3
93	CG9282	RpL24	Ribosomal protein L24	136.75	11	2
94	CG1640	CG1640	no name	136.48	7	3
95	CG1411	CRMP	Collapsin Response Mediator Protein	136.11	10	3
96	CG10712	Chro	Chromator	136.08	5	2
97	CG5695	jar	jaguar	135.55	4	3
98	CG7875	trp	transient receptor potential	134.90	3	3
99	CG17291	Pp2A-29B	Protein phosphatase 2A at 29B	133.95	7	2
100	CG3195	RpL12	Ribosomal protein L12	132.92	15	2
101	CG14648	lost	lost	131.20	7	3
102	CG17816	CG17816	no name	128.93	6	3
103	CG1539	tmod	tropomodulin	127.56	11	3
104	CG2151	trxr-1	Thioredoxin reductase-1	127.15	7	2
105	CG8495	RpS29	Ribosomal protein S29	126.10	43	3
106	CG14792	sta	stubarista	125.95	11	2
107	CG3395	RpS9	Ribosomal protein S9	125.73	23	5
108	CG3985	Syn	Synapsin	125.29	6	2
109	CG12008	kst	karst	125.10	2	5
110	CG7111	Rack1	Receptor of activated protein kinase C 1	124.59	10	2
111	CG31352	Unc-115a	Uncoordinated 115a	123.50	5	3
112	CG1725	dlg1	discs large 1	121.70	4	3
113	CG12740	RpL28	Ribosomal protein L28	120.62	22	2
114	CG8024	Rab32	Rab32	119.99	6	2
115	CG11198	ACC	Acetyl-CoA carboxylase	119.31	1	3

116	CG9075	eIF-4a	eukaryotic translation initiation factor 4A	117.29	7	2
117	CG43479	nwk	nervous wreck	116.94	3	2
118	CG15862	Pka-R2	Protein kinase, cAMP-dependent, regulatory subunit type 2	115.45	6	2
119	CG12473	stnB	stoned B	111.83	3	2
120	CG33113	Rtnl1	Reticulon-like1	106.98	15	2
121	CG10077	CG10077	no name	102.46	5	2
122	CG2139	aralar1	aralar1	101.97	4	2
123	CG10423	RpS27	Ribosomal protein S27	99.44	30	3
124	CG5812	TwdlT	TweedleT	95.96	8	2
125	CG10236	LanA	Laminin A	91.54	1	2
126	CG16885	CG16885	no name	89.03	10	2
127	CG42344	brp	bruchpilot	88.79	1	2
128	CG9412	rin	rasputin	82.00	5	2
129	CG12163	CG12163	no name	81.10	6	2
130	CG18408	CAP	CAP	79.77	2	2

Table S3. List of proteins binding to the N-terminal part of Vps13. The proteins are listed in order of decreasing PEAKS Protein Score (-10logP). The number of supporting peptides and the percentage of protein coverage are also shown.